Efficient hybrid de novo assembly of human genomes with WENGAN

Alex Di Genova, Elena Buena-Atienza, Stephan Ossowski, Marie-France Sagot

Editorial Summary: The genome assembler WENGAN produces high-quality human genome sequences at low computational cost.

Efficient hybrid *de novo* assembly of human genomes with WENGAN

Alex Di Genova[1,2,*], Elena Buena-Atienza[3,4], Stephan Ossowski[3,4] and Marie-France Sagot[1,2,*]

[1]Inria Grenoble Rhône-Alpes, 655, Avenue de l'Europe, 38334 Montbonnot, France.

[2]Université de Lyon, Université Lyon 1, CNRS, Laboratoire de Biométrie et Biologie Evolutive UMR 5558, F-69622 Villeurbanne, France.

[3]Institute of Medical Genetics and Applied Genomics, University of Tübingen, Tübingen, Germany.

[4]NGS Competence Center Tübingen (NCCT), University of Tübingen, Tübingen, Germany.

*Correspondence should be addressed to Alex Di Genova (email: digenova@gmail.com) and Marie-France Sagot (email: marie-france.sagot@inria.fr).

Generating accurate genome assemblies of large, repeat-rich human genomes has proved difficult using only long, error-prone reads, and most human genomes assembled from long reads add accurate short reads to polish the consensus sequence. Here we report an algorithm for hybrid assembly, WENGAN, that provides highest quality at low computational cost. We demonstrate *de novo* assembly of four human genomes using a combination of sequencing data generated on ONT PromethION, PacBio Sequel, Illumina and MGI technology. WENGAN implements efficient algorithms to improve assembly contiguity as well as consensus quality. The resulting genome assemblies have high contiguity (contig NG50:17.24-80.64 Mb), few assembly errors (contig NGA50:11.8-59.59 Mb), good consensus quality (QV:27.84-42.88), and high gene completeness (BUSCO complete: 94.6-95.2%), while consuming low computational resources (CPU hours:187-1,200). In particular, the WENGAN assembly of the haploid CHM13 sample achieved a contig NG50 of 80.64 Mb (NGA50:59.59 Mb), which surpasses the contiguity of the current human reference genome (*GRCh38* contig NG50:57.88 Mb).

Introduction

Genome assembly is the process by which an unknown genome sequence is constructed by detecting overlaps between a set of redundant genomic reads. Most genome assemblers represent the overlap information using different kinds of assembly graphs [1, 2]. The main idea behind these algorithms is to reduce the genome assembly problem to a path problem where the genome is reconstructed by finding "the" true genome path in a tangled assembly graph [1, 2]. The entanglement comes from the complexity that repetitive genomic regions induce in the assembly graphs [1, 2]. The first graph-based genome assemblers used overlaps of variable length to construct an overlap-graph [2]. The main goal of the overlap graph approach and of its subsequent evolution, namely the string graph [3], is to preserve as much as possible the reads information [2, 3]. However, the read-level graph construction requires an expensive all-vs-all read comparison [3]. The read-level nature implies that a path in such a graph represents a read layout, and a subsequent consensus step must be performed in order to improve the quality of bases called along the path [3]. These graph properties are the foundation of the overlap-layout-consensus (OLC) paradigm [3-5].

A seemingly counterintuitive idea is to fix the overlap length to a given size (k) to build a *de Bruijn* graph [1]. However, *de Bruijn* graphs have several favorable properties making them the method of choice in many modern short-read assemblers [6-8]. In this approach, the fixed-length exact overlaps are detected by breaking the reads into consecutive k-mers [1]. The k-mers are usually stored in hash tables (constant query time), thus avoiding entirely the costly all-vs-all read comparison [6-8]. Unlike a string graph, the *de Bruijn* graph is a base-level graph [1, 6-8], thus a path (contig) represents a consensus sequence derived from a pileup of the reads generating the k-mers (k-mer frequency). Moreover, the *de Bruijn* graph is useful for characterizing repeated as well as unique sequences of a genome (repeat graph [9]). However, by splitting the reads into k-mers, valuable information from the reads may be lost, especially when these are much longer than the selected k-mer size [3].

The type of overlap detected, and therefore the type of assembly graph constructed, is related to the sequencing technology used to generate the reads. One class of modern high-throughput sequencing machines produces short (100-300 bp) and accurate (base-error < 0.1%) reads [10, 11], and a second class produces long (>10kb) but error-prone (base-error < 15%) reads [12, 13]. Despite the high per base error rate of long-reads, the latter are the better choice for genome reconstruction [14], as longer overlaps reduce the complexity of the assembly graph [15], and therefore more contiguous genome reconstructions are achievable [14].

Independent of the sequencing technology, the goals of a genome assembler are to reconstruct the complete genome in (1) the fewest possible consecutive pieces (ideally chromosomes) with (2) the highest base accuracy while (3) minimizing the computational resources (the 1-2-3 Goals). Short-read *de Bruijn* graph assemblers are good for accomplishing goals 2 and 3 [6-8], while long-read assemblers excel at achieving goal 1 [4, 5].

Modern long-read assemblers widely adopted the OLC-paradigm [4, 5, 16-19] and new algorithms have substantially accelerated the all-vs-all read comparison [16-19]. Such progress has been possible by avoiding entirely the long-reads error-correction step [16-19], and by representing the long-reads as fingerprints derived from a subset of special *k*-mers (*i.e*. minimizers [20], minhash [19] etc.). The reduced long-read representation is appropriate for detecting overlaps >2kb in a fast way [16, 18, 19]. The newest long-read assemblers are therefore starting to be good also at goal 3 [16, 18, 19]. However, assembling uncorrected long-reads has the undesirable effect of giving more work to the consensus polisher [17, 19, 21-23]. Genome assembly polishing is the process of improving the base accuracy of the assembled contig sequences [17, 19, 21-24]. Usually, long-read assemblers perform a single round of long-read polishing [16, 18, 19], that is followed by several rounds of polishing with long [17, 19, 21, 23] and short [17, 22, 24] reads using third-party tools [17, 19, 21-24].

Currently, polishing large genomes, such as the human genome, can take much more computational time than the long-read assembly itself [16, 18, 19]. Even after several rounds of polishing, a substantial fraction of consensus errors remains, hampering the subsequent genome analyses such as gene and protein prediction [25]. Lastly, PacBio recently introduced High-Fidelity reads (HiFi reads), increasing significantly the base accuracy of long reads [26]. This technology moves the polishing bottleneck to the upfront by generating multiple error-prone reads (10 passes) of circularized fragments (10-20kb size) [26]. Each fragment is then computationally corrected to generate a single consensus long read (>10kb) with high base accuracy (base-error < 1%). To fully exploit HiFi reads, new assemblers have been developed [27, 28] that do not require a final polishing phase [28].

When this assembly approach employs short-read polishing [17, 22, 24], then it corresponds to a long-read-first hybrid assembly strategy [29, 30]. Another hybrid assembly strategy consists in starting the assembly process with short reads [31]. However, none of the described hybrid strategies employs the short-reads to tackle the problem of assembly contiguity, *i.e*. they do not aim at joining two long reads by a short-read contig, and therefore exploit only partially the short-read sequence information.

Here we introduce WENGAN, a hybrid genome assembler that, unlike most long-read assemblers, entirely avoids the all-vs-all read comparison, does not follow the OLC paradigm, and integrates short-reads in the early phases of the assembly process (short-read-first). We validated WENGAN with standard assembly benchmarks. Our results demonstrate that WENGAN optimizes the 1-2-3 Goals and is particularly effective at low long-read coverage (15X). Furthermore, we show that the WENGAN assemblies performed by combining ultra-long Nanopore reads with short or HiFi reads surpass the contiguity of the current human reference genome.

Results

The WENGAN algorithm

WENGAN starts by building short-read contigs using a *de Bruijn* graph assembler [6-8] (Figure 1.1). Then, the pair-end reads are pseudo-aligned [32] back to detect and error-correct chimeric contigs as well as to classify them as repeats or unique sequences (Figure 1.2). Repeated sequences induce complex *de Bruijn* graph topologies in their neighborhood, and short-read assemblers can choose wrong paths while traversing such complex regions, thus leading to chimeric contigs (Supplementary Fig. 1). Chimeric short-read contigs limit the accuracy and contiguity of the assembly when left uncorrected (Supplementary Fig. 2). Each short-read contig is therefore scanned base-by-base and split at sub-regions lacking pair-end read support (Supplementary Fig. 1).

Following short-read contigs correction, we generate synthetic paired-reads of different insert sizes from long-read sequences, which are mapped to the corrected short-read contigs (Figure 1.3). The spectrum of synthetic libraries is used to span the genomic repeats. For instance with ultra-long nanopore reads, we can create a spectrum composed of 24 synthetic libraries with insert sizes ranging from 0.5kb to 200kb (Supplementary Fig. 3). Matched pairs are stored with a reference to the long-read from which they were extracted (colors appearing in pairs, Figure 1.3). Using the mapped pairs and the corrected short-read contigs, we then build the Synthetic Scaffolding Graph (SSG). The SSG is an extension of the scaffolding graph [33], where there is an additional edge-labeling function that labels (colors) the SSG edges with the long-reads (Figure 1.3-4). After the SSG construction (Figure 1.4) and subsequent repeat masking (Figure 1.5), we employ the SSG to compute implicit approximate long-read multiple alignments by searching for transitive long-read-coherent paths (Figure 1.6). The aim of this graph operation (called *transitive reduction*) is to restore the full long-read information in the SSG. Each successful reduction modifies the weight as well as the shape of the SSG (Figure 1.6). After restoring the long-read information, we order and orient the short-read contigs by applying an approximation algorithm [34] that uses all the connectivity information at once to produce an optimal assembly backbone (Figure 1.7). The solution is validated by checking the distance constraints that the reduced long-read-coherent paths impose on the assembly backbone (Figure 1.8).

A property of the SSG is that all edges connecting two short-read contigs (called *mate-edges*) are spanned by at least one long-read. We therefore use the inner long-read sequence of the synthetic mate-pairs that span the mate-edge to build a long-read consensus sequence using a partial order alignment graph [17,35] (Figure 1.9). The corresponding short-read contig-ends are then aligned [36] to the mate-edge consensus sequence to determine the correct boundaries, thus filling the gap between the two short-read contigs. We computed the Pearson correlation of the mate-edge length before and after filling the gap for a total of 283,727 mate-edges. The correlation is very high ($R^2 > 0.99$) even for large gaps (>100kb, Supplementary Fig. 4).

The final steps use the SSG to polish the mate-edge consensus sequences by finding long-read-coherent paths that traverse the repeated regions (*i.e.* P4 and P6 for R1, Figure 1.10) or pairwise alignments [36]

between the repetitive short-read contigs and the mate-edge consensus sequences (Figure 1.10). Finally, the hybrid contigs are reported in FASTA format (Figure 1).

WENGAN surpasses the contiguity of GRCh38

To explore the contiguity limit of WENGAN, we assembled the human haploid cell line CHM13, which has been sequenced with a plethora of technologies including accurate short Illumina reads, long and accurate PacBio/HiFi reads [28], and ultra-long Nanopore reads [30]. In particular, the HiFi reads were generated using a large insert-size library (20 kb) at 30X of genome coverage, with half of the HiFi data (N50) contained in accurate reads larger than 17 kb (Supplementary Table 1). Similarly, the Nanopore reads were generated using an ultra-long read protocol optimized for MinION [29] resulting in 30X genome coverage by reads of at least 100 kb (Supplementary Table 1).

We generated two WENGAN assemblies, one that combines 60X of Illumina reads (2x250bp, Supplementary Table 2) with ultra-long Nanopore reads, termed WENGAN (ILL+UL), and a second one that combines both long-read technologies, termed WENGAN (HIFI+UL). The WENGAN (ILL+UL) assembly has a total length of 2.84Gb with half of the genome contained in contig sequences larger than 71.25 Mb (NG50, Figure 2A). Similarly, The WENGAN (HIFI+UL) assembly has a total length of 2.84Gb with a contig NG50 of 80.64 Mb (Figure 2A). The contig NG50 of both WENGAN assemblies exceed the contiguity of the human reference genomes GRCh37 and GRCh38 (Figure 2A and Supplementary Fig. 5).

We compared WENGAN to state-of-the-art non-hybrid long-read assemblers (Figure 2) using public assemblies generated from ultra-long Nanopore [5, 18, 19, 30] or PacBio/HiFi reads [5, 27, 28] (Supplementary Table 3, Methods: Assembly validation). These genome assemblies of CHM13 represent the quality that can be achieved using the two long-read technologies independently. In terms of assembly contiguity, the NG50 of WENGAN (ILL+UL) is almost twice as long compared to PEREGRINE (HiFi) [27] (NG50: 38.11Mb) and CANU (HiFi) [5] (NG50: 46.82Mb), is substantially longer than the assembly generated by SHASTA (UL) [19] (NG50: 58.09Mb), and has similar NG50 as the assemblies generated by FLYE (UL) [18] (NG50: 70.32Mb) and CANU (UL) [5] (NG50: 77.96Mb). The WENGAN (HIFI+UL) assembly reaches an NG50 of 80.64Mb, which outperforms all aforementioned assemblers, except for the recently developed HICANU (HiFi) assembler [28] (NG50: 82.40Mb, Figure 2A). An assessment of the assembly quality with QUAST [37] based on a whole genome alignment to the GRCh38 reference and subsequent masking of complex genomic regions (see Methods), reveals that both WENGAN assemblies have a low rate of assembly errors (avg: 107.5, Figure 2B), which is comparable or lower than its peers, except for SHASTA (78 errors). Replacing the GRCh38 reference by the curated CHM13 assembly generated by the T2T consortium (v0.7) [30] confirms the low error rate achieved by WENGAN (Supplementary Table 4).

We evaluated the consensus quality of the assemblies using an independent set of BAC sequences of CHM13 located in unique genomic regions [30] (Supplementary Table 5). Our analysis shows that WENGAN (ILL+UL) and WENGAN (HIFI+UL) assemblies achieved median consensus qualities (median QV $\geq$ 36.06 and QV $\geq$ 42.88) that exceed the base quality of Nanopore assemblers, and are comparable to the base qualities of HiFi assemblers (Figure 2C). Moreover, the WENGAN and HiFi assemblies excel at BUSCO completeness with a

recovery of at least 94.5% of the BUSCO genes (Figure 2D). In terms of computational resources, WENGAN (ILL+UL) took 1,198 CPU hours (max. RAM 646Gb, 38 hours real-time). WENGAN's runtime was at least 183 times faster than CANU's (UL) (~219,000 CPU hours) [19], while at the same time using less memory than other assemblers such as FLYE and SHASTA. Interestingly, generating HiFi consensus reads for 30X human genome coverage requires ~40,000 CPU hours [28], which is ~40 times more computationally intensive than the WENGAN (ILL+UL) *de novo* assembly. Disregarding the excessive generation time for HiFi reads, WENGAN (HIFI+UL) took 981 CPU hours (max. RAM 125Gb, 85 hours real-time), which is more efficient than HICANU (5,000 CPU hours) [28], but less efficient than PEREGRINE (58 CPU hours) [28].

We assessed the performance of the assemblers in hard-to-assemble regions such as the repeat sequences annotated in the curated CHM13 T2T-X chromosome [30], the Major Histocompatibility Complex (MHC), and Segmental Duplications (SDs). The T2T-X chromosome (154Mb, v0.7) is the first human chromosome completely assembled [30], thus useful to assess the performance of assemblers across all the repeat families. The MHC region is repetitive and highly polymorphic [29], while SDs are the most complex repeats annotated in the human genome [38] with more than 100Mb of the SD sequence composed of repeats larger than 100kb (Supplementary Fig. 6A). The T2T-X chromosome is covered by 2 and 4 contigs with a total size of 150.9 Mb and 150.56 Mb in WENGAN (HIFI+UL) and WENGAN (ILL+UL), respectively (Supplementary Fig. 7). Both WENGAN assemblies solve more than 99.6% of the total interspersed repeats annotated in the curated T2T-X chromosome, which is better or comparable to its peers (Supplementary Table 6). All evaluated CHM13 assemblies span the 4.97Mb MHC region in a single contig (Supplementary Fig. 8), with the WENGAN assemblies reaching an NGA50 of 2.8Mb (Supplementary Fig. 8). The WENGAN assemblies resolve between 168-176 BAC sequences (Supplementary Table 5), which is better than PEREGRINE (136), comparable to SHASTA (176) and lower than FLYE (253), CANU (314) and HICANU (326). While the BACs library is enriched in SDs [30], it does not represent the full range of SDs annotated in GRCh38 (175Mb). The WENGAN assemblies resolve between 60.9-65.9Mb (Figure 2E) of the SDs annotated in GRCh38 [38], which is better than PEREGRINE, comparable to HICANU and lower than FLYE, SHASTA and CANU (Supplementary Fig. 6). However, none of the assemblers resolved more than 42% of such hard-to-assemble regions, with the best performer just assembling 22% (CANU (UL): 23.4Mb) of the SDs ≥ 100kb (104.7Mb, Supplementary Fig. 6). Even with ultra-long-reads or accurate HiFi reads, a further improvement of the algorithmic approaches will be necessary to complete the assembly of SDs [38].

Overall, we demonstrated that WENGAN achieved a genome assembly quality that rivals the curated CHM13 assembly (v0.7) generated by the T2T consortium [30]. Furthermore, replacing the PacBio/HiFi reads for short reads produced a highly competitive assembly contiguity and quality.

Evaluation of assembly accuracy and contiguity using BIONANO optical mapping

We observed that the distance between the NG50 and NGA50 values increases at greater assembly contiguity ($\bar{x}$ = 39.6Mb, Figure 2A), which is likely caused by real sequence variation between the sequenced CHM13 sample and the GRCh38 reference genome. Given this limitation of the reference-based validation, we additionally used an independent *de novo* BIONANO genome map of CHM13 [30] to assess the correctness of the WENGAN assemblies. The BIONANO map is 2.97 Gb in size with 255 contigs and an N50 of 59.6 Mbp. The BIONANO map is integrated with the sequence assembly by identifying *in silico* the nicking endonuclease-specific sites on the contig sequences (*in silico* map) followed by alignment of both maps (Figure 3). Conflicts between the two maps are identified and resolved, and hybrid scaffolds are generated by using the Bionano maps to join the contig sequences and vice versa (Figure 3). A total of 72 cuts at conflicting sites were made in 32 contig sequences of the WENGAN (ILL+UL) assembly, leading to a corrected contig NGA50 of 50.73 Mb. The WENGAN (HIFI+UL) assembly after BIONANO conflicts correction has an NGA50 of 59.59Mb (52 cuts in 24 contigs). Both corrected WENGAN assemblies are more contiguous than the GRCh37 reference genome (Figure 2A). Notably, the contiguity of the corrected WENGAN (HIFI+UL) assembly surpasses the one of the GRCh38 reference genome (59.59 vs 57.88 Mb, Figure 2A). The hybrid scaffolding produced a maximum of 102 super-scaffold sequences with a total size of 2.83Gb and an N50 of at least 80Mb (Figure 3) for both WENGAN assemblies. Only 0.8% (max: 22.42 Mb) of the WENGAN sequence was not integrated into the hybrid scaffolds (short contigs). The BIONANO scaffolding of CHM13 demonstrates that both unpolished WENGAN assemblies are functional and appropriate for subsequent genome analyses.

WENGAN optimizes the 1-2-3 *de novo* assembly goals

To validate WENGAN on diploid human genomes, we assembled three human samples, HG00733, NA24385, and NA12878, which were sequenced with very long reads (Supplementary Table 1). All sequencing data were obtained from public repositories (Supplementary Tables 1 and 2). HG00733 was sequenced using the PacBio Sequel I to 90X genome coverage with N50 ≥ 33.2kb. NA24385 and NA12878 were sequenced using the Oxford Nanopore technology at 60X and 35X genome coverage and N50s of 54kb and 72kb, respectively. The sequence data of NA24385 and NA12878 were generated using an ultra-long-read protocol [29] for ONT MinION and contain at least 3.3X genome coverage in reads larger than 100 kb (Supplementary Table 1). The long-read data were combined with at least 50X of short-read coverage (pair-ends: 2x150bp or 2x250bp, Supplementary Table 2).

WENGAN was benchmarked in its three assembly modes, namely WENGANM (MINIA3 [6]), WENGANA (ABYSS2 [7]) and WENGAND (DISCOVARDENOVO [8]). We compared WENGAN to six state-of-the-art assemblers (Table 1). The list is composed of 5 long-read-only assemblers [4, 5, 16, 18, 19] and a hybrid assembler [31] (MASURCA, Table 1). All benchmarked genome assemblies were generated by the developer of the respective assembler (Supplementary Table 3). In particular, the SHASTA assemblies were generated using an independent Nanopore dataset [19], with a genome coverage of ~60X, and including at least 6X coverage of ultra-long-reads (>100*kb*).

For NA12878 (Table 1), WENGAN produced the most contiguous assemblies, with contig NG50s of 17.24, 25.99, and 35.31 Mb for WENGANM, WENGANA and WENGAND, respectively. The best long-read assembler among the four evaluated, namely FLYE (NG50 22.91Mb), is comparable to WENGANA (NG50 25.9Mb), but is surpassed by WENGAND (NG50 35.3Mb). All the other evaluated assemblers are outperformed by any WENGAN mode (NG50 >= 17.24Mb, Table 1, Supplementary Fig. 9). Moreover, WENGAN increased the contiguity of the short-read-only assemblies by a factor of 1,833X, 2,014X and 388X, for MINIA3 (NG50 9.6kb), ABYSS2 (NG50 12.9kb) and DISCOVARDENOVO (NG50 91kb), respectively (Supplementary Table 7). The WENGAND assembly of HG00733 has the fewest gaps of any PacBio CLR assembly of a human genome, with more than half of the genome contained in contig sequences at least 32.3 Mb long (Table 1, Supplementary Fig. 9), a substantial improvement in contiguity over the FALCON (NG50 22,3Mb) and SHASTA (NG50 21.7Mb) assemblies (Table 1). The WENGAND assembly of NA24385 (NG50 50.59Mb) more than doubles the contiguity of SHASTA (NG50 20.35Mb, Table 1), surpasses the contiguity of the GRCh37 reference (NG50 38.5Mb), and matches the contiguity of the GRCh38 reference (Supplementary Fig. 9).

The structural quality was determined using QUAST [37] . The WENGAN assemblies cover up to 96.3% of the reference genome with few assembled sequences (< 0.4%) unmapped to GRCh38 (Table 1, Ref. Covered% and U. length), and the contigs have fewer duplicates than the contigs of its peers (except SHASTA, Table 1, Duplication ratio). The NGA50 (which corresponds to the NG50 corrected of assembly errors) of

WENGAND (16.41-24.52 Mb) is the highest across the three assembled genomes (Table 1, Supplementary Fig. 9). For NA12878, the NGA50 of WENGAN (11.8Mb-16.41Mb) almost doubles the ones of MASURCA (5.69Mb), WTDBG2 (7.38Mb) and CANU (7.12Mb) (Table 1). Moreover, WENGAN consistently showed a lower number of assembly errors than its peers (Table 1, Supplementary Table 8). The only exception is SHASTA, a conservative assembler [19], that has a lower number of assembly errors than WENGAND on the HG00733 (107 vs. 119) and NA24385 (126 vs. 156) genomes. However, WENGAND reaches higher NGA50s than SHASTA and almost doubles the NGA50 achieved by SHASTA on the NA24385 genome (24.5 vs. 14.3 Mb, Table 1, Supplementary Fig. 9).

The consensus accuracy of genome assemblies was determined using different sequence analyses (Table 1, Supplementary Table 9). The level of polishing of the assemblies goes from none to complete (Table 1), including examples of long-read-only (SHASTA and FALCON) and hybrid (short+long reads, CANU and FLYE) polishing (Table 1). For all three genomes, WENGAN reaches a higher consensus accuracy than unpolished or long-read-only polished assemblies (Table 1). In the NA12878 genome, the hybrid polished assemblies of CANU and MASURCA have better short indel rates than the WENGAN assemblies, but WENGAN has better than or comparable medium and long indel rates (Table 1). Moreover, unlike long-read assemblers, the majority (≥73%) of the WENGAN consensus errors are located in the mate-edge consensus sequences (Supplementary Fig. 10), representing at most 10% of the WENGAN assembled sequence. The 100-mer analysis reveals that the WENGAN assemblies contain at least 84.5% of the 100-mers of the reference (Table 1). The BUSCO gene completeness of the WENGAN assemblies ranges from 94.62% to 95.20%, which is higher than the result of any other evaluated assembler and reflects the high consensus quality and contiguity of the WENGAN assemblies (Table 1). Hybrid polishing of the FLYE assembly consumed 755 CPUs hours (Supplementary Table 10). While the hybrid polishing removed millions of consensus errors (Table 1, Supplementary Table 10), and increased the median quality value and the BUSCO gene completeness (to 23.39 and 89.7%), the hybrid polished FLYE assembly still has a lower quality than any of the unpolished WENGAN assemblies (Table 1).

We analyzed how hard-to-assemble regions are resolved on these diploid human genomes (Supplementary Figures 11A and 12). WENGAN with ultra-long reads spans the MHC region with less than 4 contigs (Supplementary Fig. 11B). The top performers, namely CANU (NA12878), FALCON (HG00733), and WENGAND (NA243875), solve the MHC region in a single contig achieving NGA50s ≥ 3.5Mb (Supplementary Fig. 11B). However, all the evaluated assemblers produce a mix of haplotypes, and therefore subsequent phasing must be performed to fully solve the MHC region [29]. Regarding segmental duplications (Supplementary Fig. 12), WENGANM and WENGANA resolve over 41Mb (~6Mb of SDs > 100Kb), which is better than WTDBG2 (17Mb) and comparable to SHASTA ($\bar{x}$=42Mb, Supplementary Fig. 12). WENGAND resolves more SD sequences with ultra-long nanopore reads (56.09-60.12 Mb) and matches the top performer CANU on NA12878 (56.09 vs 56.98Mb). With PacBio reads, the FALCON assembler resolves 6.4Mb more SD sequences than WENGAND (Supplementary Fig. 12). The SD analysis of these three diploid samples shows that WENGANA and WENGANM are more conservative than WENGAND for SDs assembly, and that

WENGAND is comparable to the top performers (FLYE, CANU), while achieving a lower rate of assembly errors (Table 1, Figure 2B, Supplementary Fig. 12).

In terms of computational resources, the WENGAN assemblies consumed less than 1,000 CPU-hours (Table 1, Supplementary Table 8, max. elapsed time of 45 hours). WENGANM, the fastest WENGAN mode based on MINIA3, consumed ~738 times less CPU-hours than CANU (203 vs.~150,000 hours, Table 1) and only required 53Gb of RAM to complete the assembly (Table 1).

Collectively, the benchmark results demonstrate that WENGAN is the only genome assembler evaluated that optimizes all of the 1-2-3 *de novo* assembly goals, namely, contiguity, consensus accuracy, and computational resources.

WENGAN is effective at low long-read coverage

We investigated the required long-read coverage to produce *de novo* assemblies with NG50 of at least 10Mb. Moreover, we assessed the suitability of the BGI sequencing technology [11] (MGIseq-2000) as an alternative to Illumina SBS [10] for hybrid assembly using matched short-read genomic data. We sequenced the NA12878 human cell line using the short-read sequencers NovaSeq-6000 [10] and MGIseq-2000 [11] as well as the long-read sequencer ONT PromethION [13] (Methods section). We generated a total of 548.2 million pair-end reads (2x150bp) of sequence (53.06X) from both short-read sequencers (Supplementary Table 2). Furthermore, three flow-cells of PromethION produced a total of 10.4 million reads (40X) with a N50 of 17.18 kb (Supplementary Table 1). We randomly subsampled the long-read data from 10X to 30X of genome coverage in increasing batches of 5X. The N50 was nearly identical for all the long-read subsamples (N50 = 19.6 kb, Supplementary Table 11). WENGAN and the best long-read assembler among those evaluated, namely FLYE (v2.5), were used to build hybrid and long-read assemblies for each subsample (Figure 4, Supplementary Table 12).

A major increase in contiguity for WENGAN was observed when going from 10X to 15X of long-read coverage (Figure 4A, Supplementary Table 12). In particular, we observed an NG50 increase from 2.5, 2.9, 6.9 Mb to 7.4, 8.2, 15.5 Mb for WENGANM, WENGANA, and WENGAND, respectively. At shallow long-read coverage (10-15X), FLYE is outperformed by all WENGAN modes. Over 20X coverage, FLYE outperforms WENGANM and is comparable in contiguity to WENGANA (Figure 4). Notably, WENGAND using 15X long-read coverage leads to an NG50 of 15Mb, which FLYE can only reach at 30X long-read coverage (Figure 4A).

All assemblies generated by WENGAN cover more than 93.8% of the reference genome at any long-read coverage (Figure 4B). As expected, FLYE achieves its highest consensus quality at 30X long-read coverage (max QV=21.08, Supplementary Table 13). Polishing FLYE with long and short (NovaSeq) reads increased its median consensus quality to QV=27.21 (Supplementary Table 14). Almost all WENGAN assemblies achieve higher consensus quality than the polished FLYE assembly (min WENGAN QV=27.67 excluding WENGANA-BGI-10X, Figure 4B, Supplementary Tables 12 and 13).

The contiguity and consensus quality of the WENGAN assemblies vary more as a function of WENGAN's mode than with the type of short-read data used (Figure 4A-B). Indeed, under the same WENGAN mode, the largest difference in contiguity between the short-read technologies of Illumina and BGI is NG50=2.8Mb (WENGAND at 30X, Figure 4A) and their consensus quality is almost identical (Figure 4B). WENGANM required a maximum of 187 CPU hours (max elapsed time < 18.1 hours on 20 CPUs) and 44 Gb of RAM to complete the assemblies (Figure 4B, Supplementary Table 12). To our knowledge, this is the first time that a genome assembler reaches a contiguity of 10Mb and consensus quality of QV 29.4 on such minimal and accessible sequencing and computing resources.

We checked the assemblies of FLYE and WENGAN to see if they solved the 4.97Mb MHC region (Figure 4C). The WENGAN assemblies at low coverage (≤ 20X) reach higher NGA50 than the FLYE assemblies (Figure 4C, Supplementary Fig. 13). However, FLYE over 25X coverage assembles the MHC region in less than two contigs with a NGA50 of 4Mb (Figure 4C, Supplementary Fig. 13).

In summary, we demonstrated that WENGAN reduces the computational resources and the long-read coverage required for assembling a human genome. WENGAN produced a high quality assembly with NG50 > 10Mb (QV > 29) by combining 20X long-read coverage with 50X short-read coverage using less than one day of computing time on a low-end server (20 cores, ≤50Gb RAM).

Discussion

We have demonstrated that WENGAN is the only genome assembler that optimizes the three main goals of *de novo* assembly algorithms, namely, contiguity, consensus accuracy and computational resources. Furthermore, WENGAN is effective at shallow long-read coverage (≥15X), and in combination with ultra-long-reads generated *de novo* assemblies that surpass the contiguity of the human reference genome GRCh38. We introduced a hybrid assembly combining accurate PacBio/HiFi reads with ultra-long Nanopore reads and achieved an assembly quality that rivals the quality of the assembly generated by the T2T consortium (v0.7) [30]. Additionally, we observed no significant difference in assembly quality between using the short-read platforms Illumina NovaSeq-6000 [10] or MGIseq-2000 [11] for hybrid assembly with WENGAN. Moreover, WENGAN produces high quality assemblies with any combination of short-read (NovaSeq or MGIseq-2000) and long-read (ONT MinIon/PromethION or PacBio Sequel I) technologies.

Unlike current long-read assemblers, WENGAN generates functional and ready to use genome reconstructions. The consensus quality benchmark demonstrated that short-read polishing remains mandatory for assemblies generated from Nanopore and PacBio CLR reads (Table 1, Supplementary Tables 3, 9, and 13). Although PacBio's HiFi-reads represent an option that mitigates the post-assembly polishing, and, in combination with ultra-long Nanopore reads generates assemblies with the highest contiguity, this comes at a reduced throughput (~10 CLR reads to generate 1 HiFi read) and a substantially increased computational resources [26, 28]. We found that hybrid WENGAN assemblies provide a computationally efficient solution for human genome assembly to date, producing, at the same time, highly competitive assembly contiguity and quality.

Previous genome assemblers cannot cope with the high-throughput of a long-read and a short-read sequencer. Although other long-read-only assemblers may have a similar real-time execution [19](1 day), they require less accessible computational resources, more long-read coverage, and process half the data compared with WENGAN. Still, our analyses of hard-to-assemble regions demonstrated that further algorithmic improvements are necessary for all examined assemblers. Even though we have centered our analysis on human genomes, WENGAN also achieves high assembly quality of non-human genomes (Complete BUSCO genes ≥ 95%, Supplementary Table 15). Moreover, the WENGAN approach also provides a natural framework to combine long-read with linked-read data, and/or Sanger size short-reads [39], and/or optical maps (BIONANO), which may lead to the assembly of 'telomere-2-telomere' scaffolds without the need for extra polishing and finishing methods. Therefore, WENGAN should facilitate the democratization of *de novo* assembly of human genomes, enabling high-quality genome-assembly for many applications. The WENGAN assembler is available at GITHUB (`https://github.com/adigenova/wengan`) and CODE OCEAN (`https://doi.org/10.24433/CO.9469612.v1`).

Acknowledgements. The authors are grateful to Vincent Lacroix for helpful comments on initial versions of the manuscript. We would like to thank the NCCT members Antje Schulze Selting and Christina Engensser for excellent technical assistance.

Funding. This work was supported by INRIA and by the German Research Foundation (DFG). The genome assemblies were performed on the supercomputing infrastructure of the NLHPC (ECM-02), Chile.

Author contributions. ADG devised the original ideas for WENGAN, developed, implemented and benchmarked WENGAN. MFS guided the development of WENGAN. EBA performed sequencing of NA12878 and primary quality control of sequenced data. ADG wrote the initial version of the manuscript. MFS and SO improved initial versions of the manuscript. All authors were involved in discussions and revisions of the project and manuscript.

Competing Interests. The authors declare that they have no competing financial interests. **Correspondence**. Correspondence should be addressed to Alex Di Genova (email: digenova@gmail.com) and Marie-France Sagot (email: marie-france.sagot@inria.fr).

References

1. Pevzner, P. A., Tang, H. & Waterman, M. S. An Eulerian path approach to DNA fragment assembly. *Proceedings of the National Academy of Sciences* **98**, 9748–9753 (2001).

2. Myers, E. W. *et al*. A whole-genome assembly of drosophila. *Science* **287**, 2196–2204 (2000).

3. Myers, E. W. The fragment assembly string graph. *Bioinformatics* **21**, ii79–ii85 (2005).

4. Chin, C.-S. *et al*. Phased diploid genome assembly with single-molecule real-time sequencing. *Nature Methods* **13**, 1050–1054 (2016).

5. Koren, S. *et al*. Canu: scalable and accurate long-read assembly via adaptive k-mer weighting and repeat separation. *Genome Research* **27**, 722–736 (2017).

6. Chikhi, R. & Rizk, G. Space-efficient and exact de Bruijn graph representation based on a Bloom filter. *Algorithms for Molecular Biology* **8**, 22 (2013).

7. Jackman, S. D. *et al*. ABySS 2.0: resource-efficient assembly of large genomes using a Bloom filter. *Genome Research* **27**, 768–777 (2017).

8. Weisenfeld, N. I. *et al*. Comprehensive variation discovery in single human genomes. *Nature Genetics* **46**, 1350–1355 (2014).

9. Pevzner, P. A., Tang, H. & Tesler, G. *De novo* repeat classification and fragment assembly. *Genome Research* **14**, 1786–1796 (2004).

10. Bentley, D. R. *et al*. Accurate whole human genome sequencing using reversible terminator chemistry. *Nature* **456**, 53–59 (2008).

11. Huang, J. *et al*. A reference human genome dataset of the BGISEQ-500 sequencer. *GigaScience* **6**, 1–9 (2017).

12. Eid, J. *et al*. Real-time DNA sequencing from single polymerase molecules. *Science (New York, N.Y.)* **323**, 133–138 (2009).

13. Jain, M., Olsen, H. E., Paten, B. & Akeson, M. The Oxford Nanopore MinION: delivery of nanopore sequencing to the genomics community. *Genome Biology* **17**, 239 (2016).

14. Sedlazeck, F. J., Lee, H., Darby, C. A. & Schatz, M. C. Piercing the dark matter: bioinformatics of long-range sequencing and mapping. *Nature Reviews. Genetics* **19**, 329–346 (2018).

15. Koren, S. & Phillippy, A. M. One chromosome, one contig: complete microbial genomes from long-read sequencing and assembly. *Current Opinion in Microbiology* **23**, 110–120 (2015).

16. Ruan, J. & Li, H. Fast and accurate long-read assembly with wtdbg2. *Nature methods* **17**, 155-158 (2020).

17. Vaser, R., Sović, I., Nagarajan, N. & Šikić, M. Fast and accurate de novo genome assembly from long uncorrected reads. *Genome Research* **27**, 737–746 (2017).

18. Kolmogorov, M., Yuan, J., Lin, Y. & Pevzner, P. A. Assembly of long, error-prone reads using repeat graphs. *Nature Biotechnology* 1 (2019).

19. Shafin, K. *et al*. Nanopore sequencing and the shasta toolkit enable efficient de novo assembly of eleven human genomes. *Nature Biotechnology* 1-10 (2020).

20. Roberts, M., Hayes, W., Hunt, B. R., Mount, S. M. & Yorke, J. A. Reducing storage requirements for biological sequence comparison. *Bioinformatics* **20**, 3363–3369 (2004).

21. Chin, C.-S. *et al*. Nonhybrid, finished microbial genome assemblies from long-read SMRT sequencing data. *Nature Methods* **10**, 563–569 (2013).
22. Walker, B. J. *et al*. Pilon: An Integrated Tool for Comprehensive Microbial Variant Detection and Genome Assembly Improvement. *PLOS ONE* **9**, e112963 (2014).
23. Loman, N. J., Quick, J. & Simpson, J. T. A complete bacterial genome assembled *de novo* using only nanopore sequencing data. *Nature Methods* **12**, 733–735 (2015).
24. Warren, R. L. *et al*. ntEdit: scalable genome sequence polishing. *Bioinformatics* (2019). Btz400.
25. Watson, M. & Warr, A. Errors in long-read assemblies can critically affect protein prediction. *Nature Biotechnology* **37**, 124–126 (2019).
26. Wenger, A. M. *et al*. Accurate circular consensus long-read sequencing improves variant detection and assembly of a human genome. *Nature biotechnology* 1–8 (2019).
27. Chin, C.-S. & Khalak, A. Human genome assembly in 100 minutes. *BioRxiv* 705616 (2019).
28. Nurk, S. *et al*. HiCanu: accurate assembly of segmental duplications, satellites, and allelic variants from high-fidelity long reads. *Genome Research*. **30**, 1291-1205 (2020).
29. Jain, M. *et al*. Nanopore sequencing and assembly of a human genome with ultra-long reads. *Nature Biotechnology* **36**, 338–345 (2018).
30. Miga, K. H. *et al*. Telomere-to-telomere assembly of a complete human X chromosome. *Nature* **585**.79-84 (2020).
31. Zimin, A. V. *et al*. Hybrid assembly of the large and highly repetitive genome of *Aegilops tauschii* , a progenitor of bread wheat, with the MaSuRCA mega-reads algorithm. *Genome Research* **27**, 787–792 (2017).
32. Di Genova, A., Ruz, G. A., Sagot, M.-F. & Maass, A. Fast-sg: an alignment-free algorithm for hybrid assembly. *GigaScience* **7**, giy048 (2018).
33. Huson, D. H., Reinert, K. & Myers, E. W. The Greedy Path-merging Algorithm for Contig Scaffolding. *J. ACM* **49**, 603–615 (2002).
34. Moran, S., Newman, I. & Wolfstahl, Y. Approximation algorithms for covering a graph by vertex-disjoint paths of maximum total weight. *Networks* **20**, 55–64 (1990).
35. Lee, C. Generating consensus sequences from partial order multiple sequence alignment graphs. *Bioinformatics* **19**, 999–1008 (2003).
36. Sosic, M. & Sikic, M. Edlib: a C/C++ library for fast, exact sequence alignment using edit distance. *Bioinformatics (Oxford, England)* **33**, 1394–1395 (2017).
37. Mikheenko, A., Prjibelski, A., Saveliev, V., Antipov, D. & Gurevich, A. Versatile genome assembly evaluation with quast-lg. *Bioinformatics* **34**, i142–i150 (2018).
38. Vollger, M. R. *et al*. Long-read sequence and assembly of segmental duplications. *Nature methods* **16**, 88 (2019).
39. Drmanac, S. *et al*. CoolMPS: Advanced massively parallel sequencing using antibodies specific to each natural nucleobase. *BioRxiv* 2020.02.19.953307 (2020).

Figure legends:

Figure 1: The WENGAN algorithm. The WENGAN workflow consists of first assembling and error correcting the short-read contigs (1-2), creating a spectrum of synthetic mate-pair libraries from long-reads (3), and building of the Synthetic Scaffolding Graph (SSG, 4). The SSG is used to compute approximate long-read overlaps by building long-read-coherent paths (5-6). The long-read overlaps restore the long-read information and facilitate the construction and validation of the assembly backbone (7-8). The SSG is used to fill the gaps by building for each mate-edge a consensus sequence using the Partial Order Alignment graph (9). In the final step the SSG is used to polish the consensus sequences (10). The repeat contigs (2-10) are drawn uncollapsed to explain the WENGAN steps.

Figure 2: WENGAN assemblies of the haploid CHM13 genome. A) The barplot shows the contig NG50/NGA50 of WENGAN and other state-of-the-art long-read assemblers, as well as of the current human reference genomes. NG50 is the contig length such that using longer contigs produces half (50%) of the bases of the reference genome. NGA50 is NG50 corrected of assembly errors. NG50 and NGA50 were computed using as genome size the total contig lengths of GRCh38 (2.94Gb). B) Assembly errors predicted by QUAST using as reference GRCh38 (autosomes + X and Y). Assembly errors overlapping centromeric regions or segmental duplications were excluded from the analysis. C) Consensus quality assessment by alignment of 30 unique BAC sequences to the assembled contigs using the BACVALIDATION tool. D) Gene completeness was determined using the BUSCO tool. E) Segmental Duplications (SD) resolved by the genome assemblies. An SD is considered resolved if the aligned contig extends the SD flanking sequences by at least 50kb (See Methods section). Different CHM13 assemblers are represented using the same color across the five panels of the figure.

Figure 3: BIONANO scaffolding of the WENGAN assemblies of CHM13. We show the largest super-scaffold produced by merging the BIONANO map (BNG) and the WENGAN contigs (WG) generated by combining ultra-long NANOPORE reads (rel3) with PACBIO/HIFI (20kb) or ILLUMINA (2x250 bp) reads. The name of the scaffolded WENGAN contigs is displayed (WSC). Brackets in the contig name indicate that the contig was corrected by the BIONANO map, and the numbers are the start-stop coordinates of the error-free contig region. In parenthesis, we show the contig orientation in the super-scaffold. The white text in the alignments displays the number of nicking matching sites, the total number of nicking sites in the BNG contig, and the length in megabases of the alignment. The blue bar in the BNG contigs shows examples of joins guided by the WENGAN contigs.

Figure 4: *De novo* genome assemblies of NA12878 varying the long-read coverage and the short-read technology. A) The *de novo* assemblies were sorted by NG50 at each long-read coverage (lolliplot). We computed the NGA50 (which corresponds to the NG50 corrected of assembly errors) of each assembly using QUAST (see Methods section). B) The consensus quality (see Methods section) of each genome assembly as well as the CPU-hours required for the assembly are reported. C) The WENGAN and FLYE assemblies of the complex MHC region located in Chr6:28,477,797-33,448,354 (4.97Mb). The MHC sequence was aligned to the genome assemblies and the aligned blocks ≥ 30kb with a minimum identity of 95% were kept. The alignment breakpoints (vertical black lines) indicate a contig switch, alignment error or gap in the assembly. The assemblies of the MHC region are displayed in tracks by long-read coverage.

Tables

		NA12878							HG00733			NA24385	
		WenganA	WenganM	WenganD	MaSurCA	Canu	Wtdbg2	Flye	WenganD	Shasta	Falcon	WenganD	Shasta
Asm. stats	Contigs (>=50kb)	490	425	**364**	1,111	798	934	797	**387**	649	826	**270**	660
	T. lengh (Mb)	2,779	2,780	2,823	2,876	2,824	2,701	2,898	2,812	2,802	2,893	2,871	2,819
	NG50 (Mb)	17.24	25.99	**35.31**	8.43	10.41	11.84	22.91	**32.35**	21.71	22.33	**50.59**	20.35
Structural quality	Ref. Covered (%)	94.22	94.30	95.25	**95.80**	95.05	91.70	95.56	95.12	94.98	**96.06**	**96.36**	95.61
	Dup. ratio	1.002	1.002	1.006	1.013	1.008	**0.991**	1.025	1.004	**1.002**	1.020	1.011	**1.002**
	U. length (Mb)	5.21	**4.76**	8.63	24.68	9.42	32.13	21.29	6.96	**6.49**	15.41	10.54	**6.52**
	NGA50 (Mb)	11.82	14.34	**16.41**	5.69	7.12	7.38	12.36	**17.31**	12.99	14.61	**24.52**	14.32
	Max. aln (Mb)	45.66	75.32	72.84	32.62	34.07	70.48	**78.99**	71.03	**78.22**	71.68	75.56	**75.65**
	Asm. errors	153	**91**	158	275	194	124	177	119	**107**	198	156	**126**
C. R	CPU hours (h)	**203**	725	589	20,000	~150,000	891	5,000	936	**~768**	20,000	963	**~768**
	Max. RAM (Gb)	53	**45**	622	500	-	222	600	**644**	~966	-	**651**	~692
Consensus Accuracy													
Indels	Short (Mb)	1.99	1.72	0.85	**0.56**	0.57	27.16	37.3 / 2.65	**0.64**	3.09	1.19	**0.62**	3.38
	Rate (bp)	1,381	1,592	3,252	**4,966**	4,828	98	74 / 1,047	**4,372**	899	2,323	**4,499**	828
	Medium (Mb)	0.45	0.43	**0.29**	0.38	0.35	1.85	2.43 / 0.74	**0.27**	0.7	0.28	**0.29**	0.73
	Rate (bp)	6,049	6,358	**9,447**	7,335	7,766	1,442	1,142 / 3,753	**10,161**	3,982	10,046	**9,608**	3,817
	Long (kb)	17.95	18.73	17.74	19.21	45.96	**12.64**	15.60 / 16.49	22.9	18.13	**17.65**	24.85	**23.05**
	Rate (kb)	153	146	157	145	60	**211**	178 / 169	121	153	**157**	113	**121**
	per 100kb	102	90	53	**47**	55	1,135	1,471 / 147	**36**	141	62	**39**	152
100-mer comp. (%)		84.24	84.82	87.44	**87.54**	86.41	29.47	22.47 / 81.47	**87.45**	79.84	86.42	**88.53**	79.38
Median QV		27.84	28.41	**31.02**	27.10	28.79	17.08	16.41 / 23.48	26.42	23.36	**27.30**	-	-
Gene completeness													
BUSCO	# Complete	3,884	3,893	**3,898**	3,866	3,882	1,974	2,268 / 3,680	**3,907**	3,788	3,874	**3,904**	3,752
	% Complete	94.64	94.86	**94.98**	94.20	94.59	48.10	55.26 / 89.67	**95.20**	92.30	94.40	**95.13**	91.42

Table 1: WENGAN assemblies of the diploid NA12878, HG00733 and NA24385 genomes. Structural and consensus accuracy was determined as described in detail in the Methods section (Assembly validation). All the assemblies were built by the assembler developers. In particular, all the NA12878 assemblies were generated using the Oxford Nanopore (rel5) plus Illumina data at the assembly or polishing steps (Except WTDBG2). The CANU assembly was hybrid polished with NANOPOLISH x 2, RACON x 2, and PILON x 2. The FLYE assembly was hybrid polished with RACON x 2 and NTEDIT x 3 (Method section). The SHASTA assemblies were polished using only Nanopore reads with HELEN and MARGINPOLISH. The FALCON assembly was polished using only PacBio CLR reads with QUIVER. The WENGAN, MASURCA and WTDBG2 assemblies were not polished by external tools. The reported CPU time does not include the CPU time spent polishing the assembly with external tools. NG50 and NGA50 were computed using as genome size the total chromosome lengths of GRCh38 (3.088 Gb). Assembly errors overlapping centromeric regions or segmental duplications of GRCh38 were excluded from the analysis. The indels were called from aligned blocks ≥ 1kb at average identity ≥ 99%, and were classified according to their length into Short [1-2bp], Medium [3-50bp) and Long [>50bp]. The indel-rate was computed

448 dividing the amount of assembly sequence aligned by the number of indels called on such alignments. The
449 "indels per 100kb" is computed by QUAST from aligned blocks ≥ 0.5kb with a minimum identity ≥ 80%. The
450 100-mers completeness is the fraction of distinct 100-mers in the GRCh38 reference (2.835 Gb) that are
451 captured in the corresponding assembly. Consensus statistics before and after the polishing are included for the
452 FLYE assembly.

Online Methods

The WENGAN algorithm

Short-read assembly.

WENGAN can employ MINIA3 [6], ABYSS2 [7] or DISCOVARDENOVO [8] as the *de Bruijn* graph based short-read assembler. All three short-read assemblers are able to assemble a human genome in less than a day. MINIA3 and ABYSS2 were intended for low-memory assembly of large genomes. They are able to assemble human genomes using less than 40Gb of RAM [6,7]. MINIA3 is the fastest method, consuming less than 77 CPU hours to complete a human genome assembly (Supplementary Table 7). Its speed comes from the novel unipath algorithm BCALM2 [40] that uses minimizers [20] to compress quickly and with low memory the *de Bruijn* graph [40]. MINIA3 can be used iteratively to implement a multi-*k*-mer assembly approach. We used *k*-mer sizes of 41, 81 and 121 in all the WENGANM assemblies described (Supplementary Table 7). ABYSS2 uses a Bloom filter and rolling hash function as the main techniques to implement the *de Bruijn* graph-based assembly [7]. After filling the Bloom filter, ABYSS2 selects solid reads (that is, reads composed only of solid *k*-mers, namely those for which frequency(k) > 2) as seeds to create the unipaths. These are extended left and right by navigating in the *de Bruijn* graph until a branching vertex or a dead-end is encountered. In our benchmark tests ABYSS2 required on average 481 CPU hours to assemble a human genome (Supplementary Table 7). All the ABYSS2 assemblies were run using a Bloom Filter size of 40Gb (B=40G), four hash functions (H=4), solid *k*-mer with a minimum frequency of 3 (kc=3), *k*-mer size 96, and until the contig step only. DISCOVARDENOVO is a more specialized algorithm designed to assemble a single PCR-free paired-end Illumina library containing ≥150 base-pair reads. DISCOVARDENOVO is greedier in terms of memory than MINIA3 and ABYSS2. We observed a memory peak of 650Gb in our human assemblies (Supplementary Table 7). However, DISCOVARDENOVO better leverages the pair-end information and therefore produces the most contiguous short-read assemblies of all three tested assemblers (average contig NG50 69kb, Supplementary Table 7). All the selected short-read assemblers refine the constructed *de Bruijn* graph by removing sequencing errors and collapsing the genomic variants (SNPs, indels) to produce accurate consensus contigs [6-8].

Pair-end pseudo-alignment as building block for genome assembly.

In the same way as *k*-mers are the elemental building blocks of *de Bruijn* graph assemblers; WENGAN relies on pair-end pseudo-aligments as the elemental building blocks for the *de novo* assembly. We recently introduced an alignment-free method called FAST-SG [32] that uses unique *k*-mers to compute a pseudo-alignment of pair-end reads from long or short-reads technologies. Here, we present its successor, which we called FASTMIN-SG, which implements the same ideas of FAST-SG but using minimizers [20] and chaining with the MINIMAP2 API [41]. The uniqueness of the pseudo-alignment is now determined using the MINIMAP2 mapping quality score which gives a higher score to a primary chain when its best secondary chain has a weak pseudo-alignment.

To perform a pseudo-alignment of pair-ends from short-read sequencing technologies, we use (10,21)-minimizers for querying and indexing. We discard pair-end pseudo-alignments when one of the mates has a

mapping quality score ≤ 30 or covers ≤ 50% of the read bases. For mapping synthetic pair-ends extracted from long-read technologies, we use (5,20)-minimizers and a read length of 250 base pairs. A synthetic pair-end is a fragment of length *d* for which we have access to the long-read of origin, the position of the fragment in the long-read and the inner long-read sequence between both mates of the synthetic fragment. All the synthetic fragments are extracted from the long-reads using a moving window of 150bp in forward-reverse orientation. We create a spectrum of synthetic mate-pair libraries (Supplementary Fig. 3) by extracting pair-ends at different distances. The range of distances depends on the long-read lengths but go from 0.5kb to a maximum of 500kb with ultra-long nanopore reads. For noisy PacBio reads, we use homopolymer compressed *k*-mers [41] for indexing and querying the synthetic pair-ends. We discard synthetic pair-end alignments when one of the mates has a mapping quality score ≤ 40 or covers ≤ 65% of the synthetic read bases. The information associated to the long-read of each synthetic pair is stored in the read names for computing approximate long-read alignments later. FASTMIN-SG, like MINIMAP2, uses presets to modify multiple parameters, thus simplifying its usability. Currently, it has presets for raw PacBio reads (pacraw), HiFi reads (pacccs), raw (ontraw) and ultra-long (ontlon) Oxford Nanopore reads, and pair-ends (shortr) from short-read technologies (supporting Illumina or BGI). The pseudo-alignments are reported in SAM format.

Detection and split of chimeric short-read contigs.

The *de Bruijn* graph is complex around repeat sequences, and short-read assemblers can choose wrong paths while traversing such complex regions, thus leading to chimeric contigs (Supplementary Fig. 1). To detect potential chimeric contigs not supported by the short-reads, we map the pair-end reads back to the assembled short-read contigs using FASTMIN-SG (preset shortr). From the pair-end pseudo-alignments, we infer the average $\bar{x}$ and standard deviation σ of the insert-sizes distribution of the genomic library. Then, pair-ends mapped within contigs at the expected orientation and distance ($[\bar{x} - 2.5\sigma, \bar{x} + 2.5\sigma]$) are transformed into physical fragments. For each contig, we create an array of length equal to the contig length, and the contig fragments are used to increase the physical coverage of the contig bases. We then scan the physical coverage array base by base to detect Low Quality Intervals (LQI) that have fragment coverage below a minimum depth threshold (def:7). LQIs are classified according to their contig location as internal, start, end or whole. Finally, contigs are trimmed/split at the boundaries of the LQIs.

The Synthetic Scaffolding Graph (SSG).

We build on top of the work of Huson *et al*. [33] to extend the scaffolding graph formulation and create the Synthetic Scaffolding Graph (SSG). In brief, the contig scaffolding problem was defined by Huson *et al*. [33] as the determination of an order and orientation of a set of contigs that maximizes the amount of satisfied mate-pair links. The scaffolding graph $G=(V,E)$, with vertex set V and edge set E, is a weighted, undirected multi-graph, without self-loops [33]. Each contig C_i is modeled by two vertices (v,w) and an undirected contig-edge (e). The length of e is set to the contig length $l(C_i)$. The contig orientation is represented by associating each of the contig ends to one of the two vertices (*i.e.* $tail(C_i)=v$ *and* $head(C_i)=w$). Then traversing from $tail(C_i) \rightarrow head(C_i)$ or $head(C_i) \rightarrow tail(C_i)$ implies forward or reverse contig orientation, respectively. Now, consider a pair of mate-reads f and r originated from a synthetic mate-pair library with mean insert size $\bar{x}$, standard deviation σ and orientation forward-reverse that uniquely matches two different contigs C_i and C_j. The

uniquely mapped mate-pair induces a relative orientation and approximate distance between the two contigs. Such information is represented by adding a mate-edge *e* into the graph. The length of the mate-edge *e* is computed by subtracting from the expected mate-pair distance ($\bar{x}$) the amount of overlap that each contig has with the mate-pair considering the read mapping orientations: *l(e):=* $\bar{x} - (l(C_i) - pos_{C_i}(f)) - (l(C_j) - pos_{C_j}(r))$. Moreover, the standard deviation σ(*e*) of each mate-edge *e* is set equal to the standard deviation of the synthetic mate-pair library. If there is more than one mate-edge *e* between the same ends of two contigs C_i and C_j, we can bundle [33] the mate-edge *e* by computing from the set of mate-edges $e_1, e_2, \ldots . e_n$, the length of *e* as $l(e) \coloneqq p/q$ and its deviation as $\sigma(e) = \sqrt{1/q}$ where: $p = \sum \frac{l(e_i)}{\sigma(e_i)^2}$ and $q = \sum \frac{1}{\sigma(e_i)^2}$ [33]. Additionally, the weight *w*(*e*) of a bundled mate-edge *e* is set to $\sum_{i=1}^{k} w(e_i)$, otherwise to 1.

The **Synthetic Scaffolding Graph (SSG)** is an edge-bundled scaffolding graph *G*=(*V*,*E*), built from a **spectrum** of synthetic mate-pair libraries, where there is an edge-labelling function (*F*) that maps the long reads to the edges through the synthetic mate-pair pseudo-alignments.

Computing approximate long-read overlaps with the SSG.

Since the **SSG** is built from a spectrum of synthetic mate-pair libraries (*i.e*. 1kb to 10kb, Figure 1.3), it contains mate-edges from the short (1kb) to the long (10kb) range of connectivity (*i.e*. *e*1, *e*4, Figure 1.5). Now, consider a mate-edge *e* from *v* to *w* that are also connected by a transitive path $P = (m_1, c_1, m_2, \ldots, m_k)$ of mate-edges $(m_1, m_2, \ldots)$, contig-edges $(c_1, c_2, \ldots)$ and long-read labels $F(P) = (F(m_1), F(c_1), F(m_2), \ldots F(m_k))$. We can compute the path length *l*(*P*) and its standard deviation σ(*P*) as follows [33]: $l(P) = \sum l(m_i) + \sum l(C_i)$ and $\sigma(p) = \sqrt{\sum \sigma(m_i)^2}$. A mate-edge *e* from *v* to *w* (*i.e*. *e*4, Figure 1.5) can be transitively reduced on the path *P* (*i.e*. $P2 = (tail(c_2), e_3, c_3, e_5, head(c_4))$, Figure 1.6) if *e* and *P* have similar lengths and the long-read labels of *e* are coherent with every edge e_i of *P*: $|l(e) - l(P)| \leq 4\max(\sigma(e), \sigma(P))$ and $F(e) \subset F(e_i)\ \forall\ e_i \in P$. If this is the case, then the transitive path *P* (*i.e*. *P*2) is long-read coherent with the mate-edge *e* (*i.e*. e_i) and represents an approximate overlap of length *l*(*P*) among all the long-reads composing the mate-edge *e* (*F*(*e*)). We store the overlap information by removing *e* (*i.e*. *e*4) from the SSG and incrementing the weight of every mate-edge m_i in *P* by *w*(*e*) (*i.e*. $w(e_3, e_5) \mathrel{+}= w(e_4)$, Figure 1.6). Before starting the computation of approximate long-read overlaps, the repetitive contig-edges are masked, the mate-edges are sorted by ascending length *l*(*e*), and the set of biconnected components of the SSG is computed. The masking of repetitive contig-edges is performed by estimating the average coverage of unique genomic regions using as proxy the longest (10%), all likely to be single copy, short-read contigs (ū). Contig-edges with an average coverage $\overline{cx} > 1.5 * \bar{u}$ are masked by default. This repeat masking procedure is similar to but simpler than the A-statistic and threshold (~1.44) introduced by Myers *et al*. [3]. Transitive long-read-coherent path search takes place inside each biconnected component. In practice, we use a depth-first search algorithm to enumerate all the long-read-coherent paths of a given mate-edge *e*. At each edge extension, we extend the path only if the new added edge is long-read-coherent with the given mate-edge *e* ($F(e) \subset F(e_i)$). We stop searching when the size of a partial path *P* is larger than 80 vertices or its length is longer than expected (*l*(*P*)>*l*(*e*) and $|l(e) - l(P)| > 4\max(\sigma(e), \sigma(P))$). If there is more than one long-read-coherent path, we choose the path having the maximum number of hits from the long-reads supporting the given mate-edge *e*. For very long mate-edges ($l(e) \geq 100kb$),

we stop searching if we find more than 100 long-read-coherent paths. All the selected long-read-coherent paths are stored in a path database for later use.

The final SSG graph is created by performing first bundling and then transitive reduction (approximate long-read overlaps) of mate-edges. From now on, we will refer to this simply as the *reduced SSG*.

Generation of the assembly backbone with the SSG.

Computation of approximate long-read overlaps allows to solve the scaffolding problem using all the synthetic mate-pair libraries simultaneously. Given the reduced SSG, our goal is to determine an optimal set of vertex disjoint paths covering all the contig-edges with a maximum total weight of the mate-edges. Since this optimization problem is NP-hard, we use Edmond's maximum weighted matching approximation algorithm that guarantees to find an optimal solution with a worst-case performance ratio $r = W(S)/W(G) > 2/3$ [34]. The matching algorithm implementation is based on an extensive use of priority queues, leading to an O(V E log(V)) time complexity [42, 43]. All the contig-edges, as well as the mate-edges associated to repetitive contigs or having a weight smaller than 5, are masked during the matching cover step. After computing the matching cover, all the contig-edges are added to the matching cover solution and we use a depth-first-search approach to detect simple cycles. If such cycles are found, the set of biconnected components of the graph is computed and simple cycles are destroyed by removing the mate-edge of lowest weight in each biconnected component. In practice, the matching cover solutions contain few cycles (< 10 on human genomes) and we observed performance-ratios higher than $r > 0.8$. The set of optimal simple paths (lines or scaffolds) is what we call the *assembly backbone*.

Validation of the assembly backbone with the SSG.

We validate the assembly backbone using the physical genomic coverage obtained from the computation of the approximate long-read overlaps. The key idea is to identify suspicious mate-edges *e* (corresponding to potentially incorrect joins) not supported/covered by long-read overlaps longer than O (by default $O \geq 20kb$). We first assign genomic coordinates to each line $L_i = (c_1, m_2, \ldots m_{k-1}, c_k)$ from 1 to $l(L_i)$, taking into account the orientation of the contig-edges and the ordering and distance provided by the matched mate-edges. In a second step, all the contig-edges are converted into physical genomic fragments as well as the mate-edges spanned by long-reads longer than *O*. In a third step, if the vertices *v*,*w* of a reduced mate-edge *e* belong to the same line L_i and the length of *l*(*e*) is longer than *O*, we create a new simple path *pf* that goes from *v* to *w* in the line L_i. The new simple path *pf* is converted into a physical genomic fragment *f* only if the length of *pf* is similar to the length of the reduced mate-edge *e*, that is, if $|l(e) - l(pf)| \leq 4\max(\sigma(e), \sigma(pf))$. If that is the case, the simple path *pf* increases the physical genomic coverage of the line L_i. In a forth step, once the physical genomic coverage of all the lines L_i have been computed, we look for all the intervals inside a scaffold having a lack of physical coverage at the mate-edge locations and we tag such mate-edges as potentially erroneous joins. A line L_i is split at potential error joins only if the number of long-reads supporting the suspicious mate-edge *e* is less than *mlr* (default *mlr*≤4). In practice, we observe that the physical path coverage of human assemblies is around 20X (30X long-read coverage), thus usually less than 200 mate-edges are removed.

Gap filling with the SSG.

A property of the SSG is that all the mate-edges are spanned by at least one long-read. Therefore, after construction and validation of the assembly backbone, we proceed to create a consensus sequence for each of the matched mate-edges. We start by ordering the lines by decreasing length, which imposes a global order to the mate-edges and consequently to the long-read sequences. For each mate-edge e, we select the N best long-reads (default: 20) spanning e. The long-read selection is done by counting, with the edge-labeling function $F(e)$, the number of synthetic mate-pairs contributed by the long-read l_i to compose the mate-edge e. This means that, the more synthetic mate-pairs are contributed by long-read l_i, the greater is the confidence that the long-read l_i spans e. All the selected long-read sequences are sorted according to the mate-edges order using an external merge sort algorithm to create a long-read sequence database. Following the long-read database creation, we build a consensus sequence for each mate-edge using the partial order alignment graph [35]. For each mate-edge, we select the long-read contributing the most synthetic mate-pairs as consensus template, then the remaining long-reads spanning e are aligned to the template using a fast implementation of Myers bit-vector algorithm [36]. The long-read alignments are scanned to partition the long-reads into non-overlapping windows of size w (by default 500bp) on the template sequence. The long-read chunks that have an average identity lower than 65% are removed from the corresponding windows. The purpose is to use high-quality alignments to build the template consensus. For each window w, we call the consensus sequence using a SIMD accelerated implementation of the partial order alignment graph [17]. The mate-edge consensus is built by joining the window sequences. Finally, the corresponding contig-ends are aligned (using once again Myers bit-vector algorithm) to the mate-edge consensus sequence to determine the correct mate-edge sequence boundaries, thus filling the gap between the two contig-edges.

Polishing with the SSG.

Since not all the contig-edges are part of the assembly backbone (as is the case for the contig-edges related to repeats or short sequences), we can use them to improve the consensus base accuracy of the mate-edge sequences. To this end, we use two polishing strategies, one based on the SSG and a second based on pairwise alignments. The graph polisher uses the reduced SSG to find transitive long-read-coherent paths as before, but masking the contig-edges composing the assembly backbone. Since now we navigate on more complex parts of the SSG (unmasked repeat sequences), we limit the path search to a maximum of 5 million iterations on each mate-edge. Once a long-read-coherent path has been found, we align the contig-edges (with the proper orientation) to the mate-edge sequence using Myers bit-vector algorithm [36]. Then, the alignments are trimmed as a function of the average long-read-depth of the mate-edge consensus sequence. We thus expect a minimum identity between 80% and 99% when the average long-read-depth of the consensus sequence is between 1 and 20, respectively. If a contig-edge maps with an identity higher than the expected and the alignment covers at least 75% of the contig-edge, we replace the corresponding mate-edge aligned sequence by the contig-edge aligned sequence, thus polishing the mate-edge sequence. The alignment polisher searches for matches between the singleton contig-edges and all the mate-edge consensus sequences. In brief, we first index all the mate-edge consensus sequences using (5,17)-minimizers [20]. Minimizers are stored in a hash table and the ones having a frequency higher than 1000 are excluded. The (5,17)-minimizers of the contig-edges are scanned on the mate-edge sequence index to collect HSPs or exact (5,17)-minimizer matches. HSPs are sorted

by mate-edges and hits are identified by finding the longest strictly increasing subsequence (co-linear chain) between the contig and the mate edges. After collecting all the hits, we use a greedy algorithm to determine a layout of contig-edge hits along the mate-edge sequence. The greedy algorithm starts by sorting the contig-edge hits by number of minimizer matches and then adds the hits to the layout only if there is no overlap with a previously added hit. We then proceed as in the graph polisher to align and polish the mate-edge sequence using the best-hit layout. Finally, WENGAN outputs the sequence of each line plus the sequence of contig-edges (>5kb) not used in the polishing steps.

WENGAN assemblies of CHM13

The WENGAN (HIFI+UL) assembly of the haploid CHM13 genome was generated using the WENGANM mode. The PacBio/HiFi reads were assembled with MINIA3 using an iterative multi-*k*-mer approach with the following *k*-mer sizes: 41, 81, 121, 161, 201, 251, 301, and 351. The PacBio/HiFi reads were then included in all the subsequent WENGANM steps (Figure 1). The WENGAN (ILL+UL) assembly was generated using the WENGAND mode. The specific commands to reproduce both WENGAN assemblies are provided in the Supplementary Material (Subsection 1.2).

Assembly validation.

Genome assemblies generated by WENGAN and other assemblers were assessed by whole genome alignment to the human reference genome using the QUAST [37] (Version: 5.0.2) tool. QUAST was run with the options "–large –min-identity 80 –fragmented" using the GRCh38 (patch 19) reference (autosomes plus X and Y). Additionally, we ran a QUAST analysis using as reference the curated CHM13 assembly (chm13.draft_v0.7, 2.9384 Gb) generated by the T2T consortium [30] for all the CHM13 assemblies (Supplementary Table 4). Several assembly metrics (*i.e*. NG50, NGA50, largest alignment block, indels per 100kb, genome fraction, and others) were collected from the QUAST report. QUAST assembly errors overlapping centromeric regions or segmental duplications annotated in GRCh38 were excluded from the analysis using the script and annotation files provided by Shafin *et al*. [19] ("quast_sv_extractor.py -s empty -d GRCh38_masked_regions.bed -c centromeres.bed -q quast-all_alignments.tsv"). The procedure masked a total of 610Mb of the GRCh38 reference. Assembly errors before and after the masking of highly repetitive regions are reported. The consensus quality was determined by computing a more stringent alignment allowing a maximum of 1% divergence using MINIMAP2 [41] program (MINIMAP2 options: cxasm10 –cs -r2k), then contig-to-reference alignments longer than 1kb were scanned by PAFTOOLS (option call -l1000 -L1000) to call Single Nucleotide Variants, insertions and deletions. Additionally, we used the 100-mers completeness analysis to assess with an alignment-free method the consensus quality of the genome assemblies using the KMC [44] *k*-mer counter (Version 3.1.0). The GRCh38 (patch 19) reference genome has a total of 2,835,070,131 distinct 100-mers and those were intersected with the 100-mers of the genome assemblies using the KMC_TOOLS utility (option intersect -ci1 -cx1000). The gene completeness of the genome assemblies was assessed with the BUSCO [45] program (Version 3.0.2) using the MAMMALIA ODB9 gene set (4,104 BUSCO groups). The single plus duplicated complete BUSCO gene counts are reported. The consensus quality of the genome assemblies was determined by aligning orthogonal BAC or Fosmid sequences data (Supplementary Table 16). The statistics were computed considering fully resolved BAC/Fosmid only. The BAC/Fosmid consensus quality analysis was performed using the BACVALIDATION tool

(https://github.com/skoren/bacValidation). The amount of Segmental Duplication (SD) resolved by the genome assemblies of CHM13, HG00733, NA12878 and NA24385 was determined using SEGDUPPLOTS [38] (https://github.com/mvollger/segDupPlots). SEGDUPPLOTS aligns the assembled contigs to GRCh38 and considers an SD as resolved when the aligned contig extends the SD flanking sequences by at least 50kb. The sequence of the T2T-X chromosome was repeat-masked with the REPEATMASKER program (version 4.1.0, search engine: HMMER v3.2.1, options: "-species human -gff -xm") using the DFAM(v3.1) database. The contigs of the CHM13 assemblies were anchored to the T2T-X chromosome using MASHMAP (version v2.0) and then masked with REPEATMASKER using the aforementioned options. Finally, the WENGAN assemblies of CHM13 were validated and scaffolded using the hybridScaffold.pl program (BIONANO Solve3.4_06042019a) (with the options -c hybridScaffold_DLE1_config.xml -B 2 -N 2) and the BIONANO map assembled by the T2T-consortium [30].

Hybrid polishing of FLYE assemblies

We polished the FLYE assemblies of NA12878 using the same sequencing reads employed in the WENGAN assemblies. We used two rounds of long-read polishing with RACON [17] followed by three rounds of short-read polishing with NTEDIT [24]. The commands executed as well as the consensus quality improvement after each round of polishing are provided in the Supplementary Material (Supplementary Tables 10 and 14).

Genome sequencing of NA12878.

The genomic DNA from the GM12878 human cell line was purchased from the Coriell Institute (cat. no. NA12878, RRID:CVCL_7526).

MGI sequencing

Library preparation for the NA12878 sample was performed with the MGIEasy DNA Library Prep Kit V1.1 (MGI, 940-200022-00) following the manufacturer's instructions. Briefly, 1µg of genomic DNA at a concentration of 12.5ng/µL was fragmented with an E220 Covaris program optimized to yield fragments of 450bp average length. A double-sized selection was performed with AMPure XP beads (Beckman Coulter) at 0.52X ratio followed by a 0.15X ratio as recommended by MGI. A total of 50ng of fragmented DNA was used for the end repair and A-tailing reaction following the manufacturer's instructions. A set of adapters with 8 barcodes were ligated to the repaired DNA for one hour at 23^{o}C. After purification with AMPure XP beads (Beckman Coulter) at a 0.5X ratio, the DNA was subjected to PCR enrichment following the manufacturer's instructions. A total of 330ng of PCR product was hybridized with the Split Oligo (MGI, 940-200022-00) for the circularization step followed by digestion. Circularized ssDNA was purified with Library Purification Beads (MGI, 940-200022-00) and quantified with an ssDNA assay on a Qubit 3 fluorometer (Thermo Fisher). For the linear amplification to generate DNA nanoballs (DNBs), 75fmol of circularized ssDNA were used. The DNB library was loaded in a single lane and sequenced on a MGISEQ-2000 instrument with a paired-end modus and read length of 150bp with the MGISEQ-2000RS High-throughput Sequencing Set PE150 (MGI, 1000003981) according to (DNBs) manufacturer's instructions.

Illumina sequencing

Library was prepared using the TruSeq DNA PCR-Free Library Prep kit (Illumina, FC-121-3001) following the TruSeq DNA PCR-free reference guide (Illumina, 1000000039279v00). Briefly, 1µg of genomic DNA was used for fragmentation on an E220 Covaris to yield insert sizes of 350bp. The DNA was end-repaired, adenylated and subjected to adapter ligation as described in the reference guide. The library was quantified using the KAPA Lib Quantification Kit (Roche, LB3111) and dsDNA HS assay (Qubit). The average fragment size was estimated with a HS DNA kit (Agilent) on a 2100 Bioanalyzer (Agilent). A S2 flow cell was loaded with 2.2nM on a NovaSeq6000 instrument to generate 2x151 paired-end reads.

Oxford Nanopore sequencing

Three flow cells were run with the sample NA12878. One flow cell was loaded with a library prepared from unsheared genomic DNA. For the additional two sequencing runs, [14µg of] NA12878 genomic DNA was mechanically sheared with Megaruptor 3 (Diagenode) [at a concentration of 70 ng/µL in a volume of 200µL] with manufacturer's recommended speed to get sheared DNA with an average fragment length of 30Kb. Size selection was performed with Blue Pippin^{TM} (Sage Science) to remove fragments shorter than 10Kb using a 0.75% agarose cassette, the S1 marker and a high-pass protocol (Biozym, 342BLF7510). A further clean-up with AMPure XP beads (Beckman Coulter) on the size-selected DNA was performed at a 1X ratio for one library. Fragment size was assessed with the gDNA 165kb Analysis Kit on a FemtoPulse (Agilent) and the concentration of DNA was assessed using the dsDNA HS assay on a Qubit 3 fluorometer (Thermo Fisher). For each of the three sequencing runs, one library was prepared with the SQK-LSK109 Ligation Sequencing kit (ONT) per flow cell following the instructions of the 1D Genomic DNA by Ligation protocol from Oxford Nanopore Technologies. Briefly, 1.1 to 1.3µg of genomic DNA was used for the DNA repair reaction with NEBNext Ultra II End Repair/dA-Tailing Module (New England Biolabs, E7546S) and NEBNext FFPE DNA Repair Module (NEB, M6630S). Upon clean-up with AMPure XP beads (Beckman Coulter) at 1X ratio, the end-repaired DNA was incubated for one hour at room temperature with Adapter Mix (ONT, SQK-LSK109), Ligation Buffer (ONT, SQK-LSK109) and NEBNext Quick Ligation Module (NEB, E6056S). The ligation reaction was purified with AMPure XP beads (Beckman Coulter) at a 0.4X ratio and L Fragment Buffer (ONT, SQK-LSK109). A total of 600ng (25fmol) of the generated libraries were loaded into the flow cell (FLO-PR002) on a PromethION instrument (ONT) following the manufacturer's instructions. The Nanopore reads were base-called using GUPPY (v3.0.3) with the high accuracy FLIP-FLOP model.

Data availability

All sequence datasets and *de novo* genome assemblies described in the manuscript are publicly available through the corresponding repositories. Specific hyperlinks for the four human datasets are provided in the Supplementary Material: Supplementary Table 1 provides hyperlinks for all the long-read datasets; Supplementary Table 2 provides hyperlinks for all the short-read datasets; Supplementary Table 3 provides hyperlinks for all the *de novo* assemblies used in the benchmark; Supplementary Table 16 provides hyperlinks for the BAC/Fosmid sequences used for consensus quality assessment. The BIONANO data of CHM13 is available at `https://github.com/nanopore-wgs-consortium/CHM13`. Specific hyperlinks for the

non-human datasets are provided in the Supplementary Table 17. The supplementary files, including all the WENGAN assemblies described in the present manuscript, are available through Zenodo at `https://zenodo.org/record/3779515`. The specific commands for each WENGAN assembly are provided in the Supplementary Material (Subsection 1.2). The NovaSeq6000, MGISEQ-2000RS and PromethION sequence data of NA12878 were submitted to the Sequence Read Archive (SRA) under the BioProject PRJNA603060.

Code availability

The WENGAN code (version 0.2) used in this manuscript is freely available at `https://github.com/adigenova/wengan` and is distributed under the MIT open source license.

Methods-only references

40. Chikhi, R., Limasset, A. & Medvedev, P. Compacting de Bruijn graphs from sequencing data quickly and in low memory. *Bioinformatics* **32**, i201–i208 (2016).

41. Li, H. Minimap2: pairwise alignment for nucleotide sequences. *Bioinformatics* **34**, 3094–3100 (2018).

42. Galil, Z., Micali, S. & Gabow, H. An O(EV Log V) Algorithm for Finding a Maximal Weighted Matching in General Graphs. *SIAM J. Comput.* **15**, 120–130 (1986).

43. Dezsó, B., Jüttner, A. & Kovács, P. LEMON - an Open Source C++ Graph Template Library. *Electronic Notes in Theoretical Computer Science* **264**, 23–45 (2011).

44. Kokot, M., Dlugosz, M. & Deorowicz, S. KMC 3: counting and manipulating k-mer statistics. *Bioinformatics (Oxford, England)* **33**, 2759–2761 (2017).

45. Simão, F. A., Waterhouse, R. M., Ioannidis, P., Kriventseva, E. V. & Zdobnov, E. M. BUSCO: assessing genome assembly and annotation completeness with single-copy orthologs. *Bioinformatics* **31**, 3210–3212 (2015).

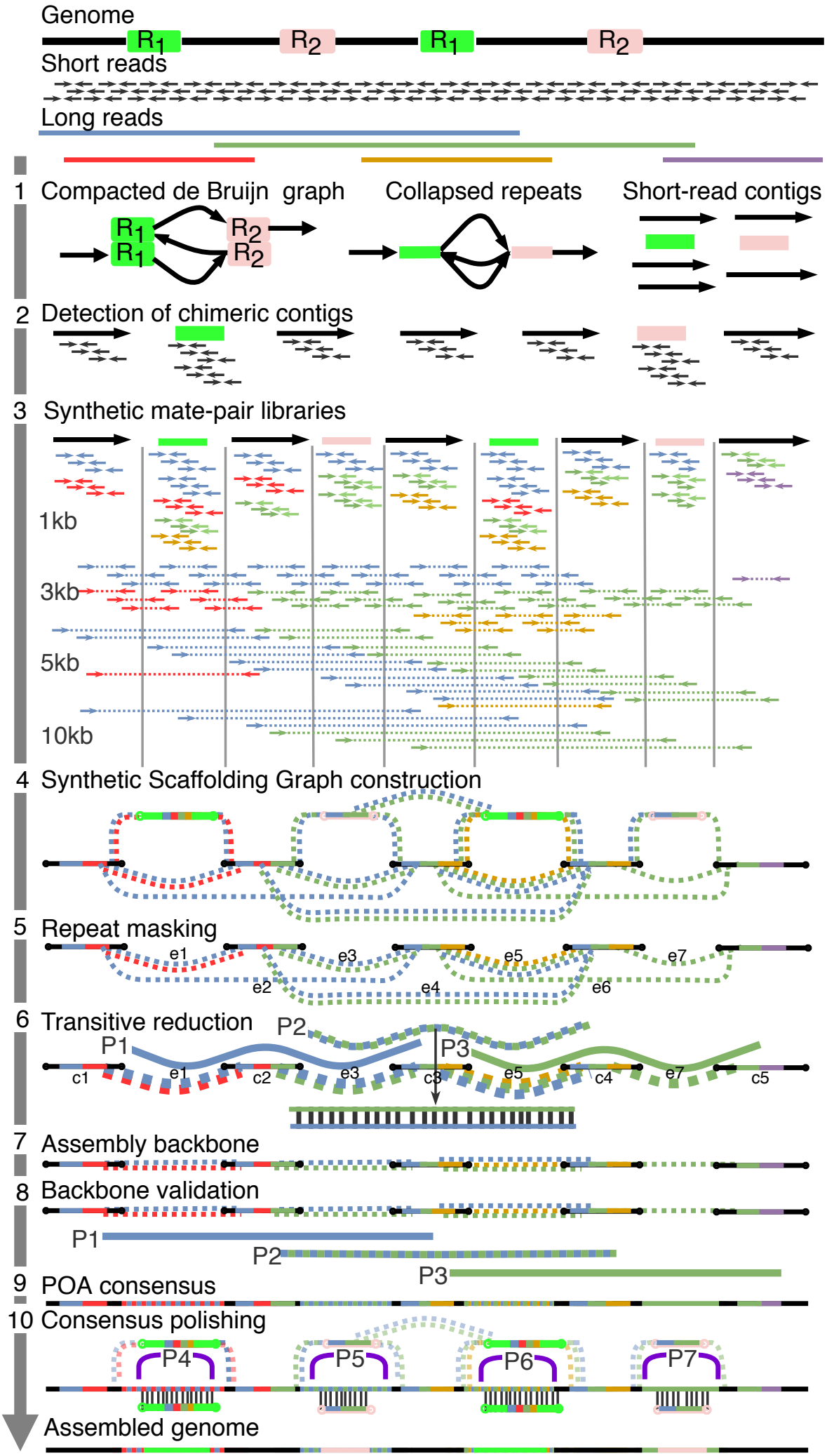
Genome
R1
R2
R1
R2
Short reads
Long reads
1 Compacted de Bruijn graph
Collapsed repeats
Short-read contigs
2 Detection of chimeric contigs
3 Synthetic mate-pair libraries
1kb
3kb
5kb
10kb
4 Synthetic Scaffolding Graph construction
5 Repeat masking
e1
e2
e3
e4
e5
e6
e7
6 Transitive reduction
P1
P2
P3
c1
c2
c3
c4
c5
7 Assembly backbone
8 Backbone validation
P1
P2
P3
9 POA consensus
10 Consensus polishing
P4
P5
P6
P7
Assembled genome

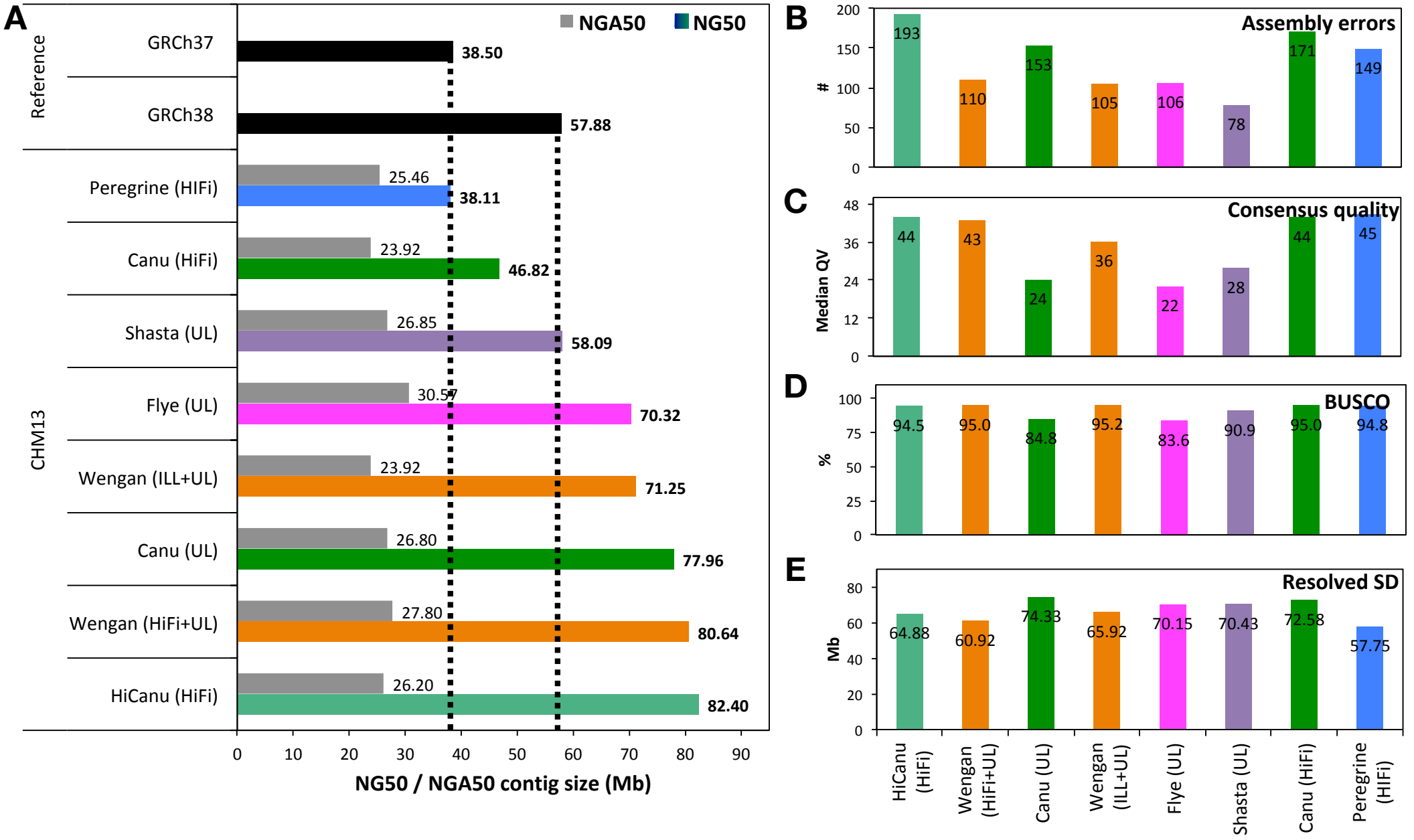
A
NGA50
NG50
Reference
GRCh37
38.50
GRCh38
57.88
CHM13
Peregrine (HIFi)
25.46
38.11
Canu (HiFi)
23.92
46.82
Shasta (UL)
26.85
58.09
Flye (UL)
30.57
70.32
Wengan (ILL+UL)
23.92
71.25
Canu (UL)
26.80
77.96
Wengan (HiFi+UL)
27.80
80.64
HiCanu (HiFi)
26.20
82.40
0 10 20 30 40 50 60 70 80 90
NG50 / NGA50 contig size (Mb)
B
Assembly errors
#
193
110
153
105
106
78
171
149
C
Consensus quality
Median QV
44
43
24
36
22
28
44
45
D
BUSCO
%
94.5
95.0
84.8
95.2
83.6
90.9
95.0
94.8
E
Resolved SD
Mb
64.88
60.92
74.33
65.92
70.15
70.43
72.58
57.75
HiCanu (HiFi)
Wengan (HiFi+UL)
Canu (UL)
Wengan (ILL+UL)
Flye (UL)
Shasta (UL)
Canu (HiFi)
Peregrine (HIFi)

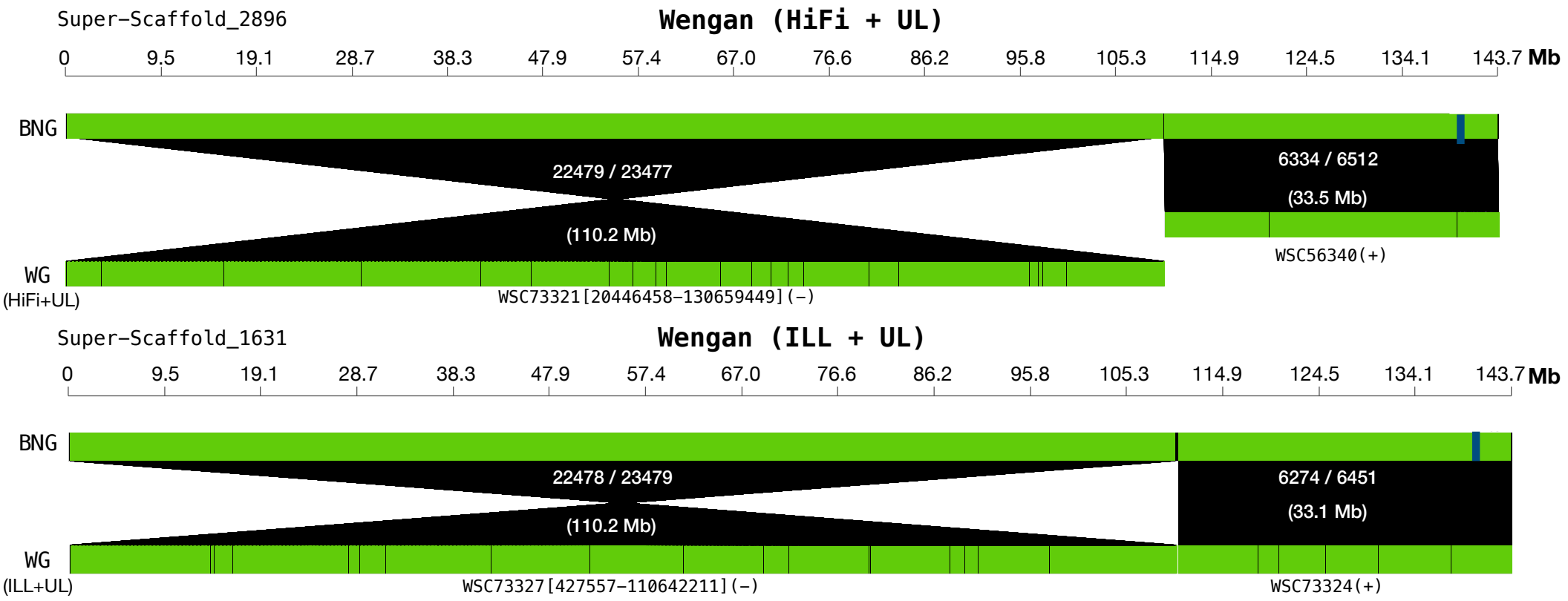
Super-Scaffold_2896
Wengan (HiFi + UL)
0 9.5 19.1 28.7 38.3 47.9 57.4 67.0 76.6 86.2 95.8 105.3 114.9 124.5 134.1 143.7 Mb
BNG
22479 / 23477
(110.2 Mb)
6334 / 6512
(33.5 Mb)
WSC56340(+)
WG
(HiFi+UL)
WSC73321[20446458-130659449](-)
Super-Scaffold_1631
Wengan (ILL + UL)
0 9.5 19.1 28.7 38.3 47.9 57.4 67.0 76.6 86.2 95.8 105.3 114.9 124.5 134.1 143.7 Mb
BNG
22478 / 23479
(110.2 Mb)
6274 / 6451
(33.1 Mb)
WG
(ILL+UL)
WSC73327[427557-110642211](-)
WSC73324(+)

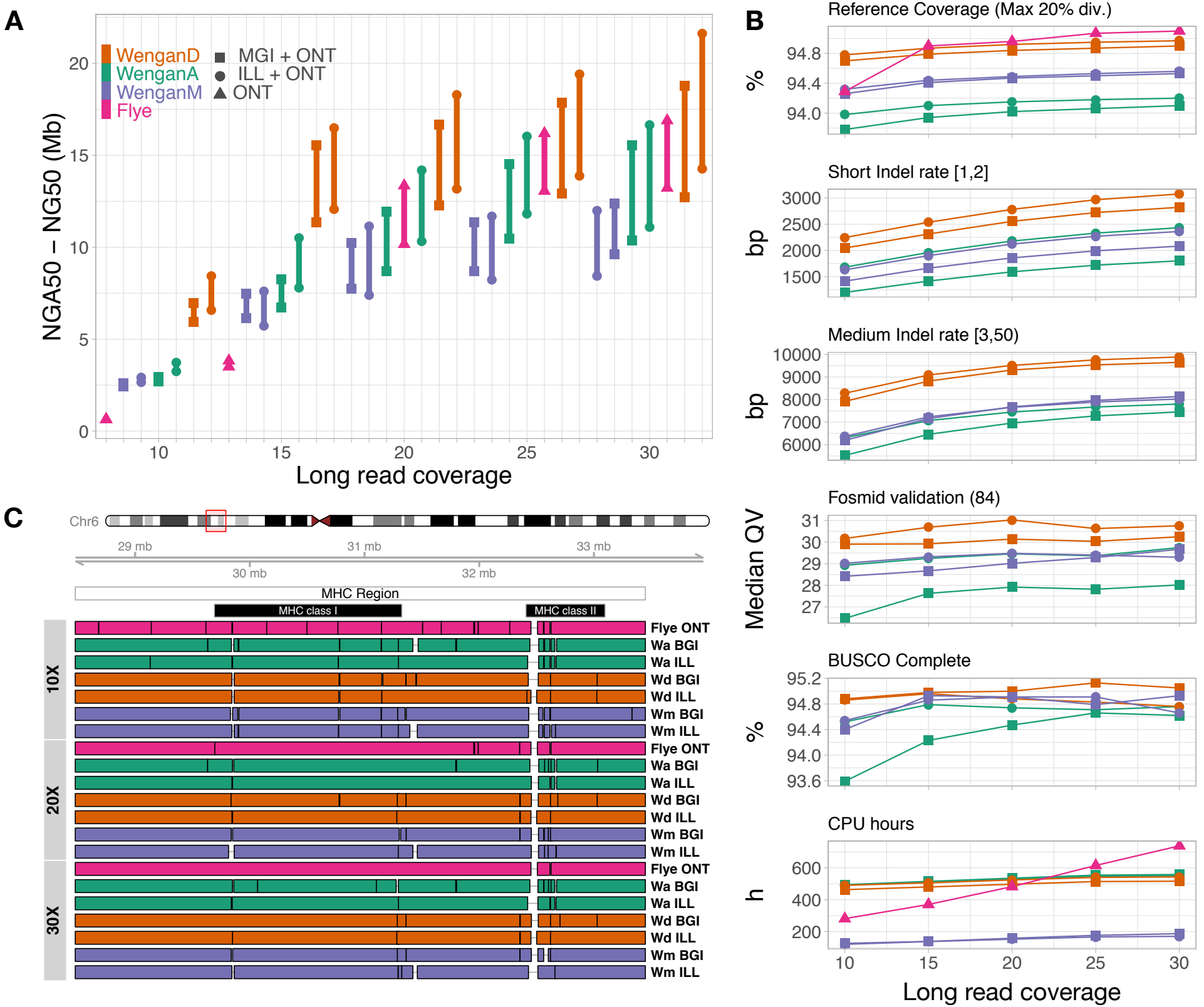
A
WenganD
WenganA
WenganM
Flye
MGI + ONT
ILL + ONT
ONT
NGA50 – NG50 (Mb)
Long read coverage
B
Reference Coverage (Max 20% div.)
%
Short Indel rate [1,2]
bp
Medium Indel rate [3,50)
bp
Fosmid validation (84)
Median QV
BUSCO Complete
%
CPU hours
h
Long read coverage
C
Chr6
29 mb
30 mb
31 mb
32 mb
33 mb
MHC Region
MHC class I
MHC class II
10X
20X
30X
Flye ONT
Wa BGI
Wa ILL
Wd BGI
Wd ILL
Wm BGI
Wm ILL